International Journal of Robotics and Control Systems
Vol. 6, No. 1, 2026, pp. 401-422
ISSN 2775-2658
http://pubs2.ascee.org/index.php/ijrcs

Enhanced Safety in Industrial Robots: An Optimized Hybrid Method for External Torque Prediction

Ikram Kouidri [a,1], Abdennasser Dahmani [b,2], Nadjem Bailek [c,d,3], Lotfi Mouni [e,4], Abdel-Nasser Sharkawy [f,g,5,*]

[a] Innovative Mechanics Laboratory (LMI), National Higher School of Advanced Technologies (ENSTA), Algiers, Algeria
[b] Department of Mechanical Engineering, Faculty of Applied Sciences, University of Bouira, Bouira 10000, Algeria
[c] Laboratory of Mathematics Modeling and Applications, Department of Mathematics and Computer Science, Faculty of Sciences and Technology, Ahmed Draia University of Adrar, Adrar 01000, Algeria
[d] Jadara University Research Center, Jadara University, Jordan
[e] Laboratoire de Gestion et Valorisation des Ressources Naturelles et Assurance Qualité, Faculté SNVST, Université de Bouira, 10000 Bouira, Algeria
[f] Mechanical Engineering Department, Faculty of Engineering, Qena University, Qena 83523, Egypt
[g] Mechanical Engineering Department, College of Engineering, Fahad Bin Sultan University, Tabuk 47721, Saudi Arabia
[1] ikram.kouidri@ensta.edu.dz; [2] dahmaniabdennasser@gmail.com; [3] bailek.nadjem@univ-adrar.edu.dz;
[4] l.mouni@univ-bouira.dz; [5] abdelnassersharkawy@eng.svu.edu.eg
* Corresponding Author

ARTICLE INFO

Article history
Received November 14, 2025
Revised January 09, 2026
Accepted February 01, 2026

Keywords
Human-Robot Interaction;
Hybrid Machine Learning;
Robotic Safety;
Particle Swarm Optimization;
External Torque Estimation;
Joint Position and Velocity;
Industrial Robots;
Data-Driven Modeling

ABSTRACT

Accurate prediction of external torque in industrial robotic manipulators remains essential for ensuring precision, operational safety, and system adaptability. The present study proposes an optimized hybrid method that accurately estimates external torque using only joint-level data, addressing the limitations of conventional approaches that rely on additional torque sensors. The performed method is the support vector machine (SVM) and its parameters are optimized using particle swarm optimization (PSO). The proposed SVM-PSO is structured based only the signals of the position sensor that is existing at any industrial manipulator joint. The developed model utilizes three input parameters: the current joint position error, the previous joint position error, and the actual joint velocity. The experimental procedures involved acquiring data under controlled sinusoidal joint motion and some random collisions with the robot links, followed by statistical validation using Williams' method to confirm the reliability of both training and testing datasets. The model demonstrated excellent performance, achieving a *RMSE* of 0.0985 and a *R* of 0.9952 during training. It maintained strong generalization performance during testing, with an *RMSE* of 0.1669 and a *R* of 0.986. The minimal discrepancy between estimated and actual external torque values affirms the method's predictive reliability. When benchmarked against existing state-of-the-art methods, the proposed approach consistently outperformed competitors in both accuracy and robustness. The elimination of external torque sensors, coupled with the exclusive reliance on joint-level data, enables a practical and scalable framework suitable for real-time torque estimation in industrial robotic systems.

1. Introduction

Currently, robotics has become necessary in many fields of life such as industry and manufacturing, agriculture, medicine, education, home and service so on, [1]-[10]. During the work of robots with environmental components to help in achieving effectively these mentioned fields, safety methods are very important and must be found and be incorporated in the robot controller, [11]-[13]. These safety methods can protect the robot itself and the interacting environment whether the human operator or any other component from accidents. These accidents may range from simple to dangerous and harmful. Estimation of the external torque of the manipulator's joint means the estimation of the external collision happened with the robot links, [14]. Therefore, a safety method can be achieved by firstly estimating the external collisions and then detecting them. The topic of this paper considers the estimation of the external joint torque (collision). Previous researchers suggested different methods for estimating the external torque of the manipulator joints. Phong et al. [15] estimated the external forces applied on the robot end-effector depending on the signal of joint torque sensors. Their method combined an estimation of time-delay and technique of input-estimation. Although their method was accurate, its application to any industrial robot is restricted since the method used a joint torque sensor which is not available in most manipulators. In [16], a Kalman filter based method was proposed by Roveda et al. for estimating the externa joint torques of the manipulator. Their method depended on the position and velocity of the manipulator joints and therefore it could be applied to any manipulator. However, the main restrictions of using Kalmen filter are stability and noise issues. Likar and Žlajpah [17] proposed a method to estimate the external joint torque and contact based on the joint torque sensors. Therefore, the application of their method is restricted to robots that have the torque sensor. In addition, they investigated their method with only robots which have links with cylindrical shape. Huo et al. [18] estimated and modulated the external force considering observer-dependent adaptive force control. Their investigation and experiments incorporated admittance and impedance controllers and disturbance observer-based approaches.

Machine learning based approaches were used for estimating the external joint torques of the manipulator. In [19], Dimeas et al. developed a fuzzy system to estimate the external torque of the manipulator joints. Their system was dependent on the joint torque sensors which are not found on most robots. In addition, their work was based on the implementation of a fuzzy system for each manipulator joint which leads to complexity if applied to more than 2-DOF manipulators. Sharkawy et al. [20] designed a coupled and decoupled neural network to estimate the external torque of 3-DOF manipulator joints. The coupled neural network achieved higher accuracy, and less complexity compared with the decoupled one. Although the high accuracy of their system, their system could be applied only to manipulators where joint torque sensors are available. In [21], Mahmoud et al. used the recurrent neural network for the estimation of the external torques of 3-DOF manipulator joints. Their system was based on the signal of the joint positions and velocities and therefore their approach could be applied to any industrial robots. In [22], Zhang et al. used a back-propagation neural network for the estimation of the external torque of the manipulator joints. The training of their method was dependent on data extracted from a torque sensor and therefore, their method applied when the torque sensor is found. They compared their approach with a momentum observer-based approach which proved the high accuracy of their new approach.

Based on the study, predicting the external torque of the manipulator joints is crucial for ensuring robotic safety. Further investigation and analysis of novel methods should be conducted. A method based on only position sensors needed to be designed to allow its applicability to any robot or any industrial robot. The number of inputs required by the method should be minimized to reduce complexity and computational load. Furthermore, the method's high accuracy should be a primary consideration by minimizing the values of MAE, MSE, and RMSE and increasing the value of regression or correlation coefficient (R). The main novelties and contributions of the current study are outlined in the following points:

1) Development of an enhanced hybrid modeling approach: This work focuses on developing an enhanced hybrid modeling approach to improve accuracy, robustness, and adaptability in robotic systems. The used method is the SVM and its parameters are optimized using PSO optimization.

2) Minimal sensor dependency: The proposed method relies solely on joint position and velocity as inputs, making it applicable to a wide range of robots and manipulators. The simplicity of the inputs also minimizes computational complexity.

3) Realistic experimental validation: Test data are collected through robot experiments involving deliberate collisions, creating a range of signal conditions to evaluate the method's ability to accurately estimate external torque across various scenarios.

4) Application or use: The proposed method can be used or applied with any industrial or conventional robot which contains only a position senor at each joint.

The following sections of the paper are discussed as follows. Section 2 shows materials and methods in which the estimation of the external torque from the dynamic equation is presented. The properties and the structure of the SVM are presented. Furthermore, the experimental work procedures that are performed with the robotic manipulator and the data that is extracted from the experiment. In Section 3, the experimental results are presented and also compared with other previous studies. In Section 4, small discussion is performed for these obtained results. Section 5 summarizes the main points in the paper and mentions some future work.

2. Materials and Methods

In this section, the dynamic modelling of the robotic manipulator, the proposed SVM and PSO optimization, the experimental work procedures, and the dataset collection and division are discussed in details.

2.1. The Dynamic Model of Manipulator

The external torque acting on the manipulator joints, denoted as Ext_T, can be calculated using the following dynamic equation [23], [24]:

$$Ext\_T = I(\theta)\ddot{\theta} + C\left(\theta, \dot{\theta}\right)\dot{\theta} + V(\theta) - T \quad (1)$$

Where:

- $I(\theta)$: Inertia matrix of the robotic manipulator
- $C(\theta, \dot{\theta})$: Coriolis and centrifugal force matrix
- $V(\theta)$: Gravity vector
- T: Actuator torque
- $\theta, \dot{\theta}, \ddot{\theta}$: Joint positions, velocities, and accelerations, respectively

However, the estimation of dynamic parameters such as $I(\theta)$, $C(\theta, \dot{\theta})$, and $V(\theta)$ is often subject to uncertainty. Accurately determining these values becomes particularly challenging in complex manipulators, such as those with six or seven degrees of freedom 6-DOF or 7-DOF, [25]-[29]. Consequently, relying solely on Equation (1) for estimating external torque may compromise both the effectiveness and efficiency of the system.

Machine learning-based approaches, particularly those grounded in data, have demonstrated high efficiency in addressing the inverse dynamics problem [30]-[32]. In this paper, an SVM-based approach is adopted to effectively estimate the external torques of manipulator joints, overcoming the limitations of traditional dynamic modeling. The proposed SVM is structured based only three inputs as follows:

1) The position error of the manipulator's joint.

2) The previous position error of the manipulator's joint.

3) The actual velocity of the joint.

The actual position of the manipulator's joint is obtained from the position sensor which is existing at the joint of the manipulator. Then, the position error is calculated by subtracting the actual position from the desired position. The actual velocity is obtained by numerical differentiation of the joint's position. As the industrial robot includes only a position sensor at each joint, therefore, the application of this SVM method could be executed in any industrial robot. The proposed structure of the SVM with PSO optimization is presented in Fig. 1.

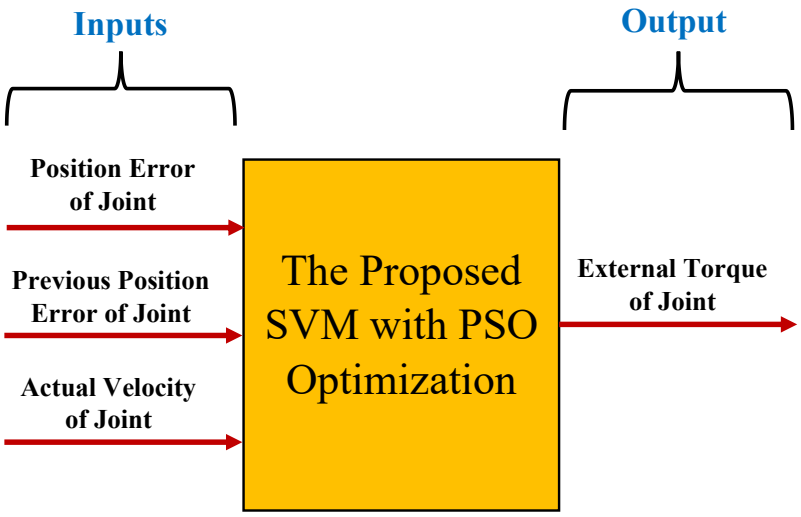

Fig. 1. The proposed structure of the SVM with PSO optimization for estimating the external torque of manipulator's joint

2.2. SVM Properties and Structure

Support Vector Machine (SVM) is a machine learning technique employed to estimate the external torque of manipulator joints. It is capable of modeling complex, nonlinear relationships between inputs and outputs, [33], [34]. In the context of torque estimation, SVM is particularly effective, leveraging historical data and a diverse range of variables to provide accurate predictions [35]-[37]. SVM comprises a set of supervised learning strategies designed to address classification, distinction, and regression problems. Its growing popularity stems from its ability to efficiently handle large datasets. The technique achieves nonlinear decision boundaries by mapping input vectors into a high-dimensional feature space and then applying a linear model to derive a separating hyperplane. This is achieved using kernel functions within the framework of SVM regression [38], [39].

A visualization of how SVM is used in regression problems whether with linear and nonlinear relationships is presented by Beny Maulana Achsan [40] and is shown in Fig. 2, [40]. The visualization presented in Fig. 2 considers the epsilon-intensive band which develops a tolerance margin for a predicted or forecasted function. The points captured inside the hyperplane's limits have the lowest error. All blue points have zero or lowest errors.

The inputs/outputs nonlinear relationship is used with regression function. The outputs of the SVM model are obtained by the following equations [41], [42]:

$$f(x_i) = w^T \emptyset(x_i) + b \tag{2}$$

Where:

- $f(x_i)$: Predicted output for input x_i.
- $\phi(x_i)$: Nonlinear function that transforms input data into a higher-dimensional feature space.
- w^T: Weight vector, representing the sensitivity of features in the high-dimensional space.
- b: Bias term in the SVM model.
- $i = 1,2,\ldots,n$: Index for each sample in the dataset, where n is the total number of samples.

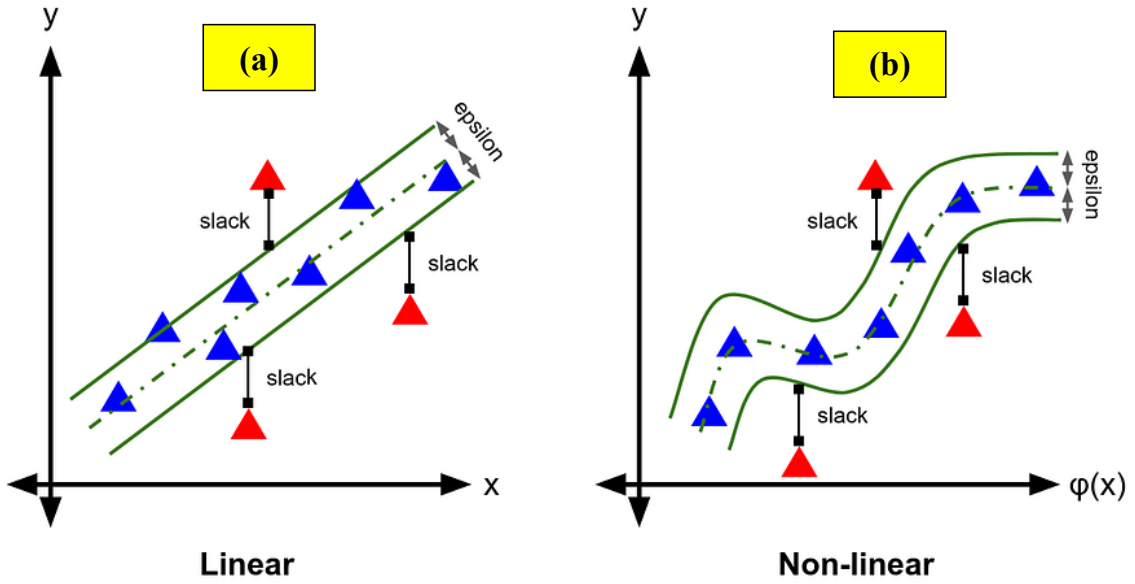

Fig. 2. SVM for linear and nonlinear regression, [40]

The dataset consists of input vectors $x_i \in \mathbb{R}^D$ and corresponding scalar outputs $y_i \in \mathbb{R}$, where D is the number of input features. The SVM optimization problem for training is defined as follows:

$$\begin{cases} min\, R(w,\xi,\xi^*,\varepsilon) = \frac{1}{2}\|w\|^2 + C\left[v\varepsilon + \frac{1}{N}\sum_{i=1}^{N}(\xi_i + \xi_i^*)\right] \\ subjective\ to:\ y_i - w^T\varphi(x_i) - b \le \varepsilon + \xi_i \\ w^T\varphi(x_i) + b - y_i \le \varepsilon + \xi_i \\ \xi^*, \varepsilon \ge 0 \end{cases} \tag{3}$$

Where:

- $\frac{1}{2}\|w\|^2$: This part defines the norm of vector of weight or the term of regularization.
- C: The parameter that makes balance between the complexity of the model and the empirical risk $\|w\|^2$.
- ξ_i^*: The slack variable for denoting the i^{th} sample's distance outside of ε-*tube*.

As the optimization problem is nonlinear and constrained, the above main problem is resolved by the construction of the dual optimization problem depending on techniques of Lagrange multipliers:

$$\begin{cases} max\, R(a_i,a_i^*) = \sum_{i=1}^{N} y_i(a_i,a_i^*) - \frac{1}{2}\sum_{i=1}^{N}\sum_{j=1}^{N}(a_i,a_i^*)(a_j,a_j^*)K(x_i,x_j) \\ subjective\ to:\ \sum_{i=1}^{N} y_i(a_i,a_i^*) = 0 \\ 0 \le a_i, a_i^* \le C/N \\ \sum_{i=1}^{N}(a_i + a_i^*) \le C.v \end{cases} \tag{4}$$

With:

- $K(x_i,x_j)$: Represents the kernel function satisfying the condition of Mercer's.
- a_i and a_i^*: Lagrange multiplier nonnegative.

$$\hat{y} = f(x_i) = \sum_{i=1}^{N} (a_i - a_i^*) K(x - x_i) + b \, , i = 1,2, \dots, n \tag{5}$$

2.3. Particle Swarm Optimization (PSO)

Particle Swarm Optimization (PSO), [43]-[45], a well-established technique for parameter optimization, is employed in this study alongside SVM to fine-tune its parameters. PSO is a nature-inspired evolutionary algorithm originally modeled on the collective behavior of bird flocks during foraging. In this framework, each bird is represented as an individual agent, or "particle," which collaborates with others in the swarm using swarm intelligence to identify the optimal solution within a defined search space [46]. In a D-dimensional optimization problem, a swarm of m particles explores the solution space. Each particle, denoted as $X_i = (x_{i1}, x_{i2}, ..., x_{iD})$, represents a potential solution. The position and velocity of each particle are updated iteratively according to the following equations:

$$v_{id}^{t+1} = w v_{id}^{t} + c_1 . r_1 . (p_{id} - x_{id}^{t}) + c_2 . r_2 . (p_{gd} - x_{id}^{t}) \tag{6}$$

$$x_{id}^{t+1} = x_{id}^{t} + v_{id}^{t+1} \tag{7}$$

Here, $V_i = (v_{i1}, v_{i2}, \dots, v_{iD})$ denotes the velocity vector of the $i-th$ particle, $P_i = (p_{i1}, p_{i2}, \dots, p_{iD})$ is the best-known position of that particle, and $P_g = (p_{g1}, p_{g2}, \dots, p_{gD})$ is the global best position found by the entire swarm. The variables c_1 and c_2 are acceleration coefficients, while r_1 and r_2 are random numbers between 0 and 1. The inertia weight (w) helps balance global and local exploration capabilities.

Due to its capability to handle continuous optimization problems and perform multi-point searches effectively, PSO is employed in this study to optimize the SVM parameters, thereby enhancing the model's predictive performance. Fig. 3 presents a flowchart illustrating the process of optimizing a SVM model using the PSO algorithm. The procedure involves data normalization, PSO initialization, iterative fitness evaluation, parameter updating, and concludes with the final training and evaluation of the optimized SVM model .The optimization focused on two key hyperparameters: the penalty parameter C, ranging from 0.1 to 100, which balances training accuracy and model generalization; and gamma, ranging from 0.01 to 1, which determines the reach of a single training point's influence in the RBF kernel. The MATLAB function fitrsvm was employed to implement and train the regression SVM based on these parameters.

The PSO algorithm was configured with a swarm size (num_particles) ranging from 3 to 30 and up to 100 iterations (max_iter) to explore the solution space. Each particle represents a candidate solution with two dimensions corresponding to the parameters C and gamma. The search is constrained within defined lower and upper bounds ([0.1, 0.01] to [100, 1]). The algorithm's behavior is governed by the inertia weight (w), which controls momentum, as well as the cognitive (C1) and social (C2) coefficients, which guide the particles toward their personal and global best solutions. Each particle's position and velocity are updated iteratively based on the swarm's performance. The fitness of each solution is evaluated using the RMSE, which quantifies the prediction error-lower values indicate better performance. Through this approach, the PSO efficiently navigates the parameter space to find optimal SVM configurations for accurate estimating the external joint torque. The optimal applied parameters are listed clearly in Table 1.

2.4. Evaluation Metrics

In this study, the Williams method, based on the leverage approach, was utilized to detect potential outliers by analyzing residuals in conjunction with the Hat matrix. The Hat matrix was calculated using the following standard formulation [47], [48]:

$$H = X(X^T X)^{-1} X^T \tag{8}$$

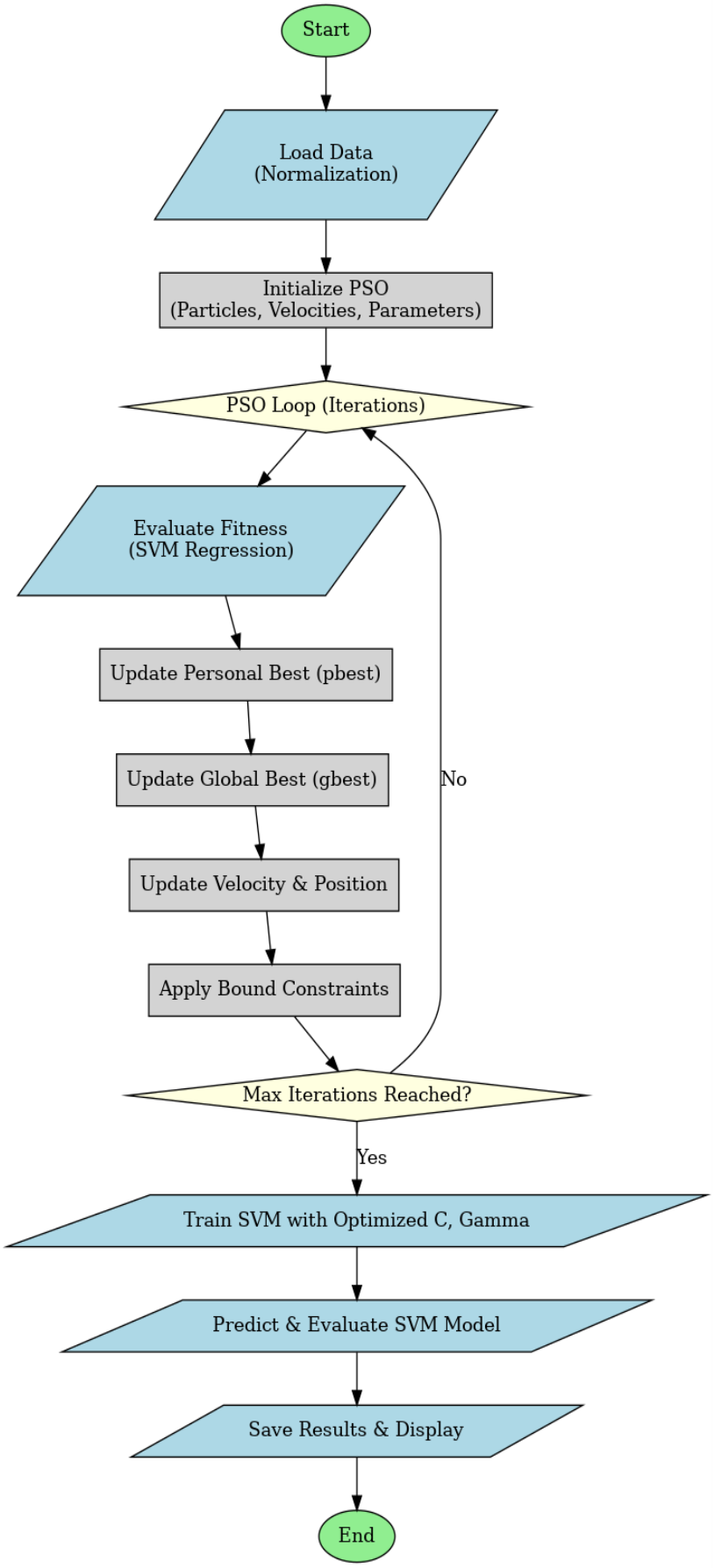

Fig. 3. Flow diagram for proposed development

Table 1. Optimal parameters applied

Parameter / Variable	Value / Range
C	96.49
gamma	0.0441
gbest_idx	10
Iteration	05
num_particles	30
lb (Lower Bounds)	[0.1, 0.01]
ub (Upper Bounds)	[100, 1]
w	0.7

Here, X denotes the $m \times n$ input matrix, where m is the number of samples and n is the number of input features used in the model. The leverage values-referred to as Hat values-are extracted from the diagonal elements of the matrix H:

$$Hat = \text{diag}(H) \tag{9}$$

To visualize the influence and error distribution of the data points, a Williams plot was generated. This diagram charts the standardized (normalized) residuals against their corresponding Hat values, making it an effective tool for detecting outliers and influential data. The critical leverage threshold (H^*) is typically defined as:

$$H^* = \frac{3(n+1)}{m} \tag{10}$$

Normalized residuals were computed by comparing experimental torque values with those predicted by the Proposed model, using the formula:

$$(R_{\text{Norm}})_i = \frac{(T_i^{\text{exp}} - T_i^{\text{cal}})}{\sqrt{\text{Var}(T^{\text{exp}} - T^{\text{cal}})}} \quad \text{for } i = 1, \ldots, m \tag{11}$$

To evaluate the accuracy of the estimating model, various error metrics were employed. Precisely, the Correlation Coefficient (R) and Root Mean Squared Error (RMSE) were utilized, as defined by following equations (12) and (13), [49], [50]. These error measures provide a comprehensive evaluation of the Support Vector Machines - Particle Swarm Optimization used to estimate the external torque of the manipulator joints, offering insights into the strengths and limitations of the proposed approach.

$$R = \frac{\sum_{i=1}^{n} \left(Y_{i,exp} - \overline{Y_{i,exp}}\right)\left(Y_{i,cal} - \overline{Y_{i,cal}}\right)}{\sqrt{\sum_{i=1}^{n} \left(Y_{i,exp} - \overline{Y_{i,exp}}\right)^2 \sum_{i=1}^{n} \left(Y_{i,cal} - \overline{Y_{i,cal}}\right)^2}} \tag{12}$$

$$RMSE = \sqrt{\frac{\sum_{i=1}^{n} (Y_{i,cal} - Y_{i,exp})^2}{n}} \tag{13}$$

Where, n: is the number of data points; $Y_{i,exp}$ and $Y_{i,cal}$ are the experimental and calculated data points of the external torque of the manipulator joints, respectively; and $\overline{Y_{i,exp}}$ is the mean experimental data.

2.5. Experimental Work Procedures

In this subsection, the experimental set-up with the robotic manipulator is discussed and how the data is collected. These data are used for phases of training and testing of the proposed method. KUKA LWR collaborative robot is used for executing experiments. The main parts of KUKA robot unit are presented in Fig. 4, [51], which contains the robot itself, the teach pendant, and the robot controller. The KUKA robot controller can give every 0.001 seconds signals like the actual position of the robot

joints, the desired position of the robot joints, measured joint torque, and the external torque of the robot joints. These parameters are very important to the proposed method which is designed using only three inputs: the position error, the previous position error, and the velocity of the joint. The main reason to use these only variables is to simulate the application of the method to industrial manipulator which has only position sensor at its joint. The position error is calculated as the difference between the desired position and the actual position. The joint velocity is calculated by determining the numerical differentiation of the position of the joint. The position error and joint velocity is presented from the following equations:

$$Position\ Error = \theta_{desired} - \theta_{actual} \tag{14}$$

$$Joint\ Velocity = \frac{d\theta}{dt} = \frac{\Delta\theta}{\Delta t} \tag{15}$$

Where, t represents time in seconds.

As the proposed method is dependent on only the position and velocity signals, therefore, it can be applicable to any industrial robotic manipulator.

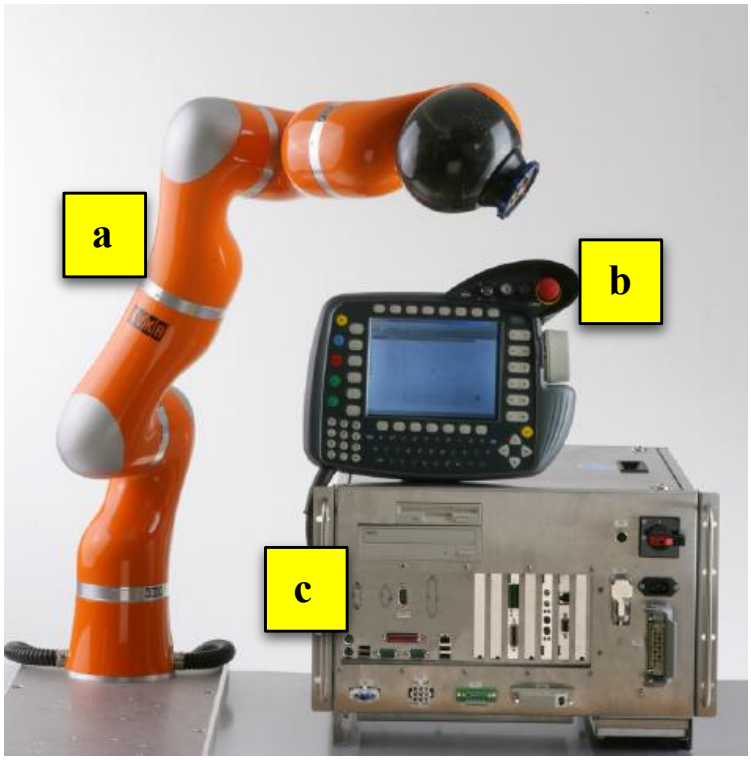

Fig. 4. KUKA LWR robot unit, [51]. (a) KUKA LWR robot, (b) The teach pendant (c) Robot controller

The experiment is developed by activating only the joint E1 of KUKA robotic manipulator, as shown in Fig. 5. The other joints of the robot are fixed. Then, commanding a sinusoidal motion to this joint. During the motion of the manipulator, the hand of the human operator does some different collisions with the robot links. The main objective of doing these collisions is to present the proposed method in estimating different conditions and situations. When the experiment is finished, the data is collected to train and to test the proposed method. This data is presented in Fig. 6 and Table 2. These data are the inputs and the outputs of the SVM which are used for the phases of training and then testing. The inputs of SVM are three variables which are the position error, previous position error, and velocity of the joint. The output of the SVM is the external torque of the joint. Fig. 7 shows clearly the data division. The total number of samples that are collected from the experiments with the robot is 25000 samples. From these samples, 20000 samples are used for training and testing our proposed SVM as follows: 14000 samples for training phase and 6000 samples for test phase.

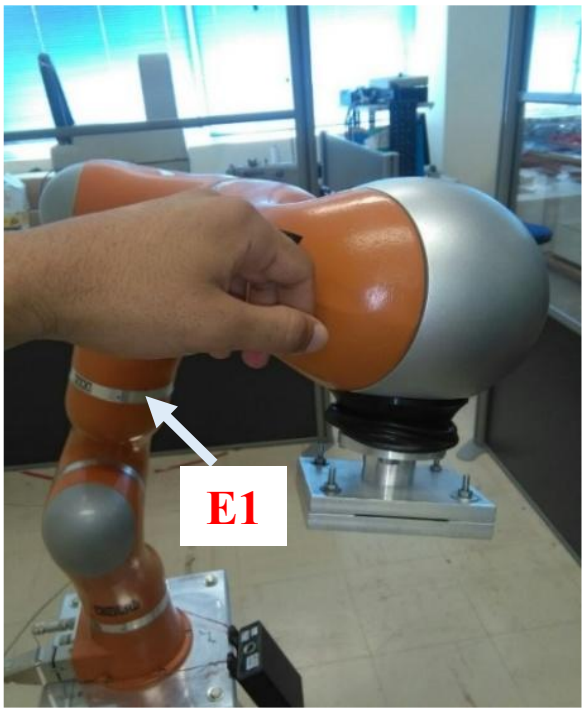

Fig. 5. The experimental set-up with KUKA robot. Only joint E1 of the robot is activated. The other joints are deactivated

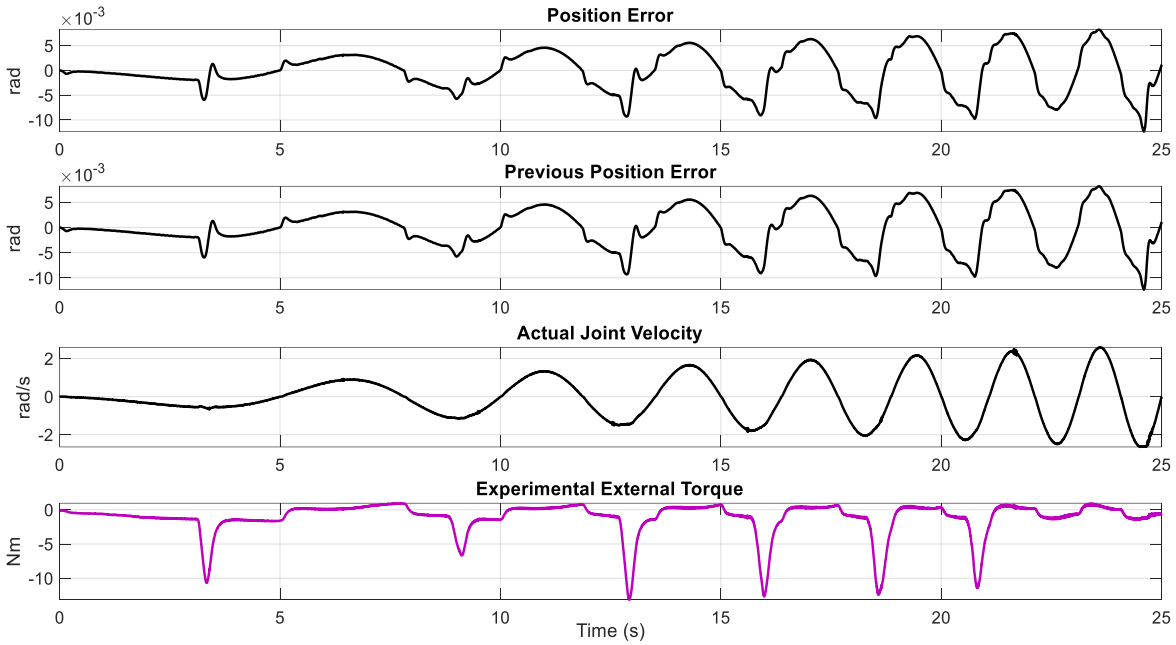

Fig. 6. The extracted data from the experiment with the robot. The spikes in the curves present the performed collisions with the robot link

2.6 Collected Data Analysis

The correlation matrix presented in Table 3 offers a clear overview of the relationships between joint motion parameters and external torque in a robotic system. The current and previous position errors exhibit a perfect positive correlation (r = 1), indicating the continuity and interdependence of joint control signals over time. Furthermore, the current position error shows a moderate correlation with actual joint velocity (r = 0.760), suggesting that positional deviations are closely linked to the joint's movement speed. A similar correlation is found between the previous position error and joint velocity (r = 0.761), reinforcing this relationship.

Table 2. Samples from the gathered data during the experimental with the robot

Samples No	Current Position Error of Joint	Previous Position Error of Joint	Actual Joint Velocity	Experimental External Torque
1	-5.25e-06	0	0	-0.12892048
2	-5.45e-06	-5.25e-06	0	-0.12768002
3	-5.72e-06	-5.45e-06	0	-0.12658548
4	-6.07e-06	-5.72e-06	0	-0.12707548
5	-6.49e-06	-6.07e-06	0	-0.12696700
…	…	…	…	…
2000	-0.00123906	-0.00123945	-0.34260747	-1.1474484
2001	-0.00124151	-0.00123906	-0.34004447	-1.1568344
2002	-0.00124675	-0.00124151	-0.33745167	-1.1710118
2003	-0.00125217	-0.00124675	-0.33748147	-1.1766193
2004	-0.00125787	-0.00125217	-0.33748147	-1.1709762
2005	-0.00126129	-0.00125787	-0.33998486	-1.1536795
…	…	…	…	…
10100	0.00259185	0.00258529	0.18787383	-0.58521307
10101	0.00259900	0.00259185	0.18918513	-0.56914222
10102	0.00260675	0.00259900	0.19061564	-0.55874044
10103	0.00261426	0.00260675	0.19288062	-0.54599017
10104	0.00262356	0.00261426	0.19299982	-0.53751439
10105	0.00262952	0.00262356	0.19824503	-0.53491658
…	…	…	…	…
24996	0.00094187	0.00091124	-0.0500679	-0.58980125
24997	0.00097275	0.00094187	-0.04088878	-0.61826873
24998	0.00100148	0.00097275	-0.02944469	-0.63808805
24999	0.00103056	0.00100148]	-0.02038479	-0.64308608
25000	0.00106037	0.00103056	-0.01168251	-0.63776147

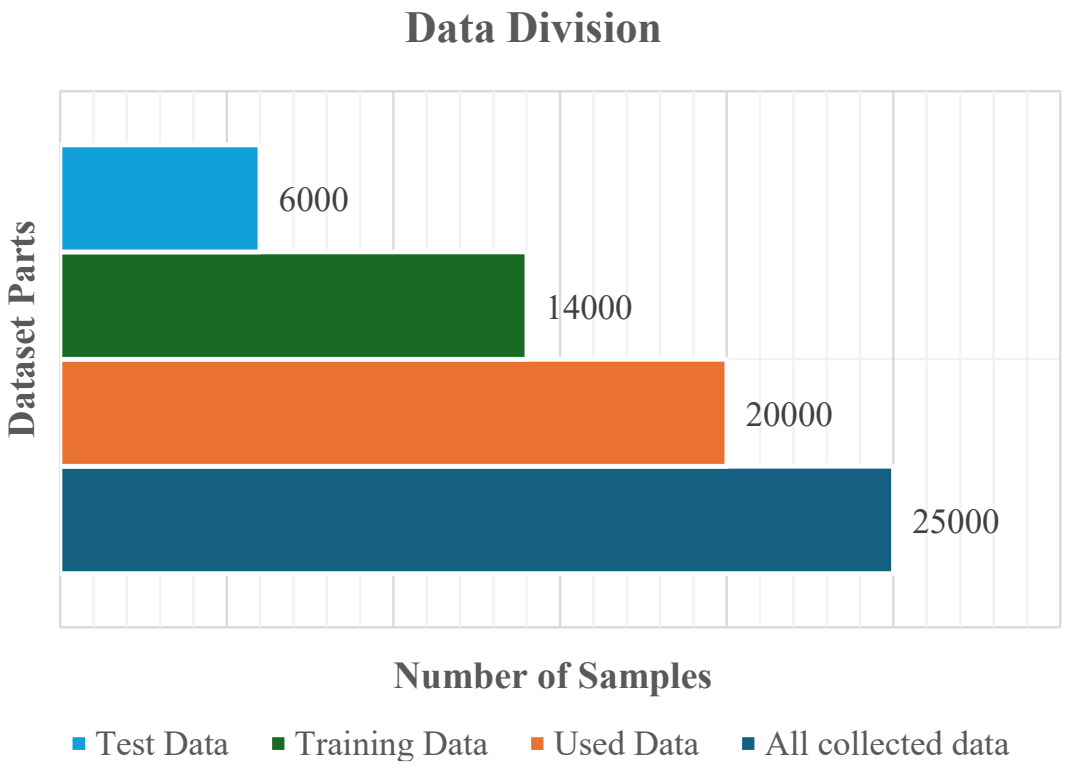

Fig. 7. The collected dataset division for the train and test phases of the proposed SVM

In contrast, the correlations between these variables and the experimentally measured external torque are noticeably weaker. For instance, external torque has only a moderate correlation with joint velocity ($r = 0.500$), and even lower correlations with the current ($r = 0.351$) and previous ($r = 0.352$) position errors. These weaker relationships imply that, although torque is partially influenced by position and velocity, other dynamic or external factors likely contribute as well.

Table 3. The correlation matrix between the three inputs and the output (external torque) of the proposed approach

Correlation	Current Position Error of Joint	Previous Position Error of Joint	Actual Joint Velocity	Experimental External Torque
Current Position Error of Joint	1	1	0.760	0.351
Previous Position Error of Joint	1	1	0.761	0.353
Actual Joint Velocity	0.760	0.761	1	0.500
Experimental External Torque	0.351	0.353	0.500	1

3. Experimental Results

This section presents the statistical results using Williams' method and the results from training and testing the SVM-PSO. Comparing the results of the current study with other previous studies is presented also in this section.

3.1. Williams' Method Results

First, we applied a Williams plot analysis to assess the statistical validity of our model's predictions. This plot demonstrates the statistical reliability and applicability domain of the developed model by analyzing both validated and suspect data points (Fig. 8). It effectively distinguishes validated predictions (left side) from those that may be extrapolated or prone to outliers (right side). The majority of data points (approximately 95%) fall within the acceptable leverage threshold of $H^* = 0.0008$ and within the standardized residual bounds of ±3. Most standardized residuals for the validated data are concentrated around zero, ranging approximately from –5 to +20, indicating strong model performance. However, a few outlier points exceed the upper standardized residual limit, even within the lower leverage region (Hat < 0.0008). This suggests that while these compounds exhibit typical structural features, the model still struggles to predict their outcomes accurately.

Next, the Williams plot analysis for the testing dataset, shown in Fig. 9, demonstrates excellent model generalization, with statistical performance metrics closely paralleling those observed in the training set. Out of 6,000 testing data points, 5,709 compounds (95.15%) fall within the validated data region, maintaining standardized residuals within the ±3 range indicated by the red horizontal lines. The remaining 291 data points (4.85%) are classified as suspect due to residual values exceeding the ±3 threshold; these outliers are mainly concentrated in the low-leverage region (hat values < 0.001) and display standardized residuals ranging approximately from –15 to +15. Overall, the distribution pattern in Fig. 9 shows that most validated data points are densely clustered near zero standardized residuals, with leverage values predominantly below 0.001, indicating robust predictive accuracy within the model's applicability domain.

3.2. SVM-PSO Training and Testing Results

Then, we carried out a scatter-plot analysis to demonstrate the correlation between actual experimental data and the predicted values generated by the proposed model during the training phase (Fig. 10). The data points are densely distributed along the ideal prediction line (shown in red). The majority of the data points cluster tightly around this ideal line across the entire range of torque values. The scatter pattern reveals minimal deviation from the ideal prediction line. While some scattered points exhibit slight deviations from the perfect correlation line, these outliers represent a small fraction of the total dataset and do not significantly impact the overall model performance. Additionally, to gain further insight into the spatial distribution of prediction errors throughout the learning process, we plotted the error value across the entire training dataset as presented in Fig. 11. The error value is determined by subtracting the predicted external torque from the actual external torque. The error values are predominantly clustered near zero throughout the training sequence, with the majority of errors falling within the ±0.5 range, demonstrating the model's consistent accuracy and high performance during the training phase.

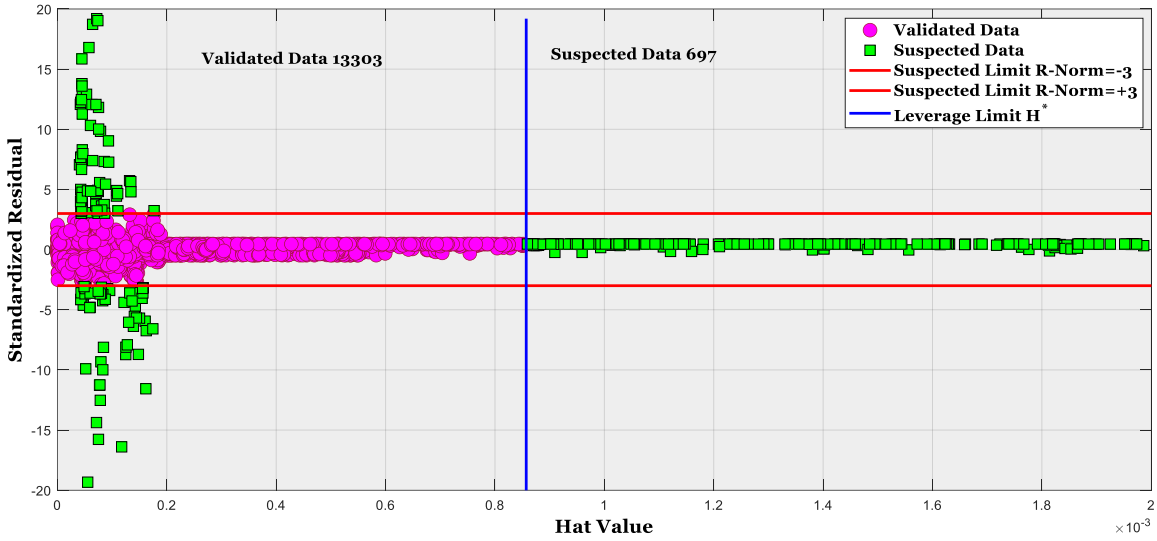

Fig. 8. Statistical validation plot for training dataset predictions

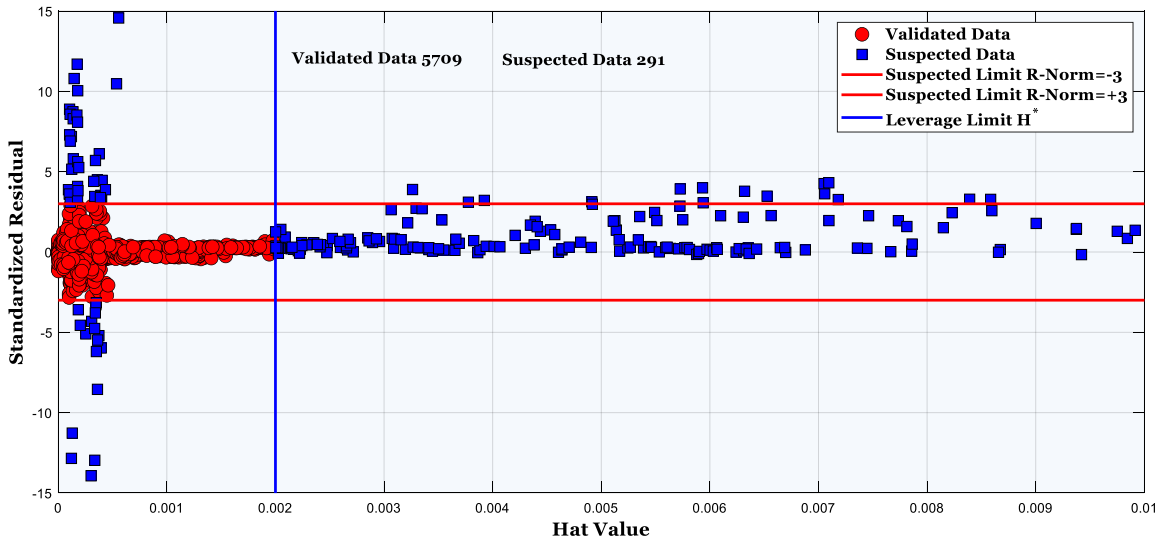

Fig. 9. Statistical validation plot for testing dataset predictions

To further explore the model behavior beyond the error values distribution, we now turn to a comprehensive performance summary: a quantitative assessment of the proposed model's performance across both the training and testing phases is provided in Fig. 12 and Table 4, using some critical statistical metrics. The R demonstrate exceptional model accuracy, with the training phase achieving R = 0.9952 and the testing phase maintaining a remarkably high R = 0.9862. This slight decrease of 0.009 between training and testing phases indicates minimal overfitting, suggesting that the model successfully generalizes to unseen data while retaining approximately 97.26% of the variance explanation capability during testing compared to 99.04% during training.

The other agreement vectors are approaching ideal conditions [i.e., $\alpha = 1$ (slope), and $\beta = 0$ (intercept)] for both phases. During the training phase, the SVM-PSO model yielded $[\alpha, \beta] = [0.9821, -0.0080]$, while in the testing phase, it produced $[\alpha, \beta] = [0.9761, -0.0163]$. The slope ($\alpha$) remains close to 1 in both phases, indicating a strong linear correlation between the estimated and actual values. In the testing phase, α remains nearly 1, further confirming the consistency and reliability of the model's estimates. However, the intercept (β) slightly deviates from the ideal value of 0 in both phases, suggesting a minor systematic bias.

After that, the MAE analysis reveals consistently low error magnitudes across both phases, with the training phase exhibiting MAE = 0.0384 and the testing phase showing MAE = 0.0551. The

increase of 0.0167 in MAE from training to testing represents a 43.5% relative increase, yet the absolute values remain exceptionally small, indicating that the average prediction error remains well within acceptable engineering tolerances. This performance metric demonstrates that the model maintains practical accuracy for real-world applications, with average deviations remaining below 0.06 units across all operating conditions.

Table 4. Best results for SVM with particle swarm optimization during training and testing phases

Phase	R	α	β	MAE	RMSE	MSE
Training phase	0.9952	0.9821	-0.0080	0.0384	0.0985	0.0097
Testing phase	0.9862	0.9761	-0.0163	0.0551	0.1669	0.0279

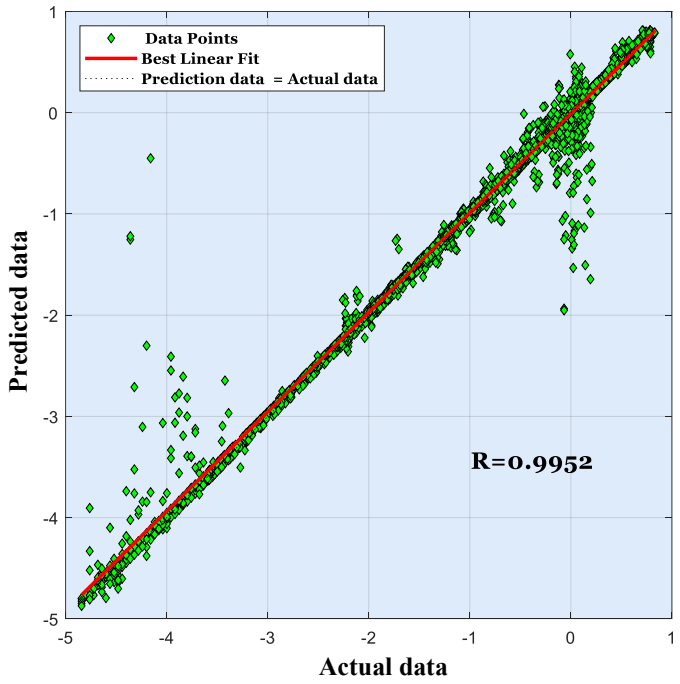

Fig. 10. Scatter plot showing prediction accuracy of the proposed model during training phase

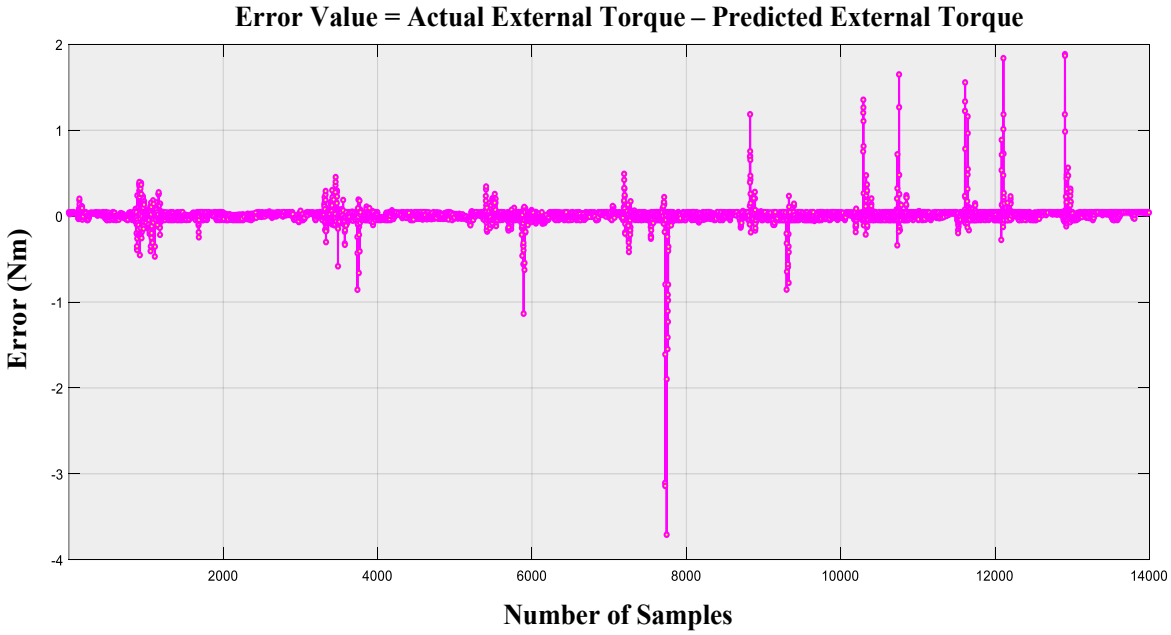

Fig. 11. The error value resulted from training phase

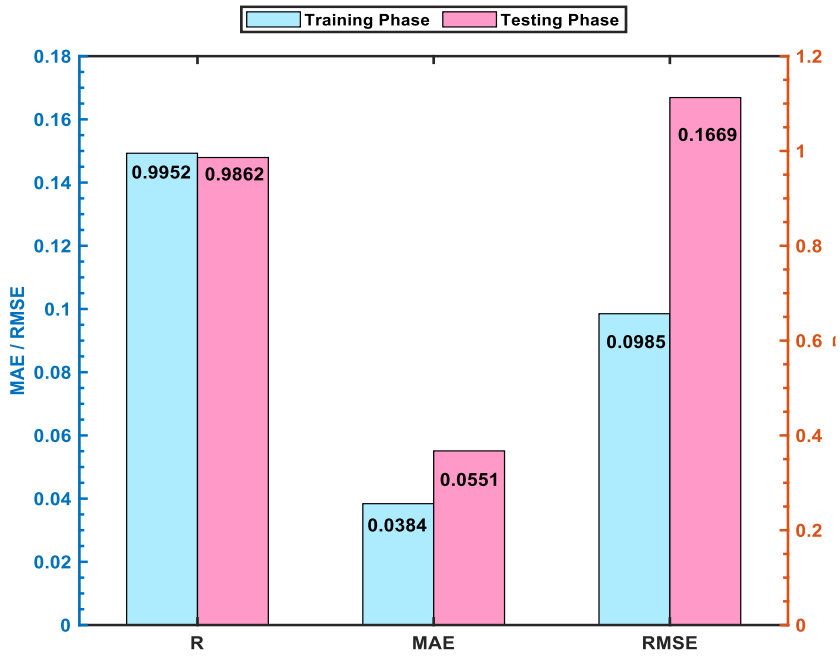

Fig. 12. The optimal values of R, MAE, and RMSE resulted SVM with particle swarm optimization during training and testing phases

The RMSE comparison provides insight into the model's handling of larger prediction errors, with training phase RMSE = 0.0985 and testing phase RMSE = 0.1669. The RMSE increase of 0.0684 from training to testing (approximately 69.4% relative increase) is more pronounced than the MAE increase, suggesting that while most predictions remain highly accurate, the model occasionally produces larger errors during testing. However, both RMSE values remain below 0.17, indicating that even the worst-case prediction errors are contained within reasonable bounds. The consistently low error metrics across all three performance indicators confirm the robustness and reliability of the proposed external torque estimation method, making it suitable for high-precision manipulator control applications where accurate torque prediction is critical for safe and effective operation. Furthermore, Fig. 13 illustrates the proposed model's exceptional predictive performance during the testing phase, providing crucial validation of the method's generalization capabilities. The comparison between actual data and predicted data across all testing points reveals remarkable agreement, with both signals exhibiting virtually identical temporal patterns and amplitude characteristics.

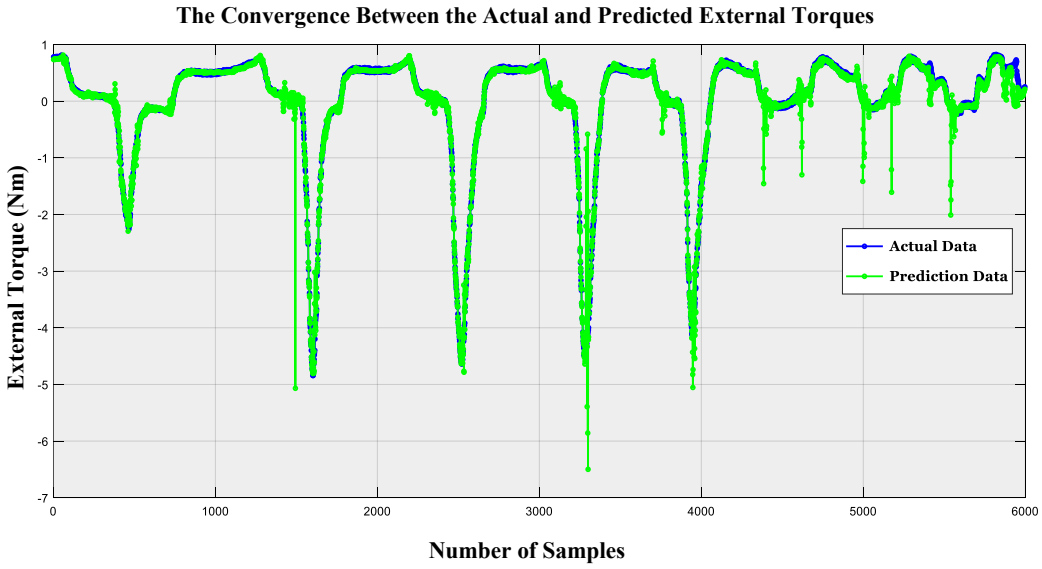

Fig. 13. Comparison between experimental (actual) and estimated external torques in the testing phase

3.3. Comparison with Other Previous Studies

Finally, we performed a detailed comparison of the proposed external torque estimation method against seven established approaches from recent literature, as presented in Table 5. The quantitative performance comparison highlights the proposed method's superiority across multiple evaluation metrics. Specifically, the present approach achieves a 69% lower MSE and a higher correlation coefficient compared to Mahmoud et al. [21], who reported an MSE of 0.03173 and $R = 0.96797$. Similarly, the proposed technique reduces errors by approximately 72% compared to Sharkawy et al. [20], whose method yielded an MSE of 0.034677. While G. d'Addato et al. [52] reported a cascaded neural network with a notably low MSE of 2.2470×10^{-4}, direct comparison is complicated due to differences in data scaling and measurement units, underscoring the need for standardized benchmarking in future research. In addition to statistical accuracy, practical applicability is a crucial consideration for industrial deployment. Among the methods compared, only four, including the present work, are suitable for use with any industrial robot without requiring specialized sensors. Within this sensor-free category, the proposed model offers the most balanced and superior performance across all evaluation criteria. In summary, the proposed method's combination of high predictive accuracy, sensor independence, and broad industrial compatibility makes it a highly practical, scalable, and efficient solution for external torque estimation in real-world manufacturing environments.

Table 5. Comparison between the current results with other previous approaches

Authors	Prediction Variable	Model Type	Evaluation Index	Application (+)
The Proposed Study	External torque of the manipulator joints	SVM with PSO Optimization	R = 0.9862 MSE = 0.0097 RMSE = 0.0985	Any industrial robot
Dimeas et al. [19]	External Torque Estimation	Fuzzy System	MSE is not stated. Average errors = 0.03 and 0.01 Nm	Torque sensor is required which is not available in industrial robots.
Sharkawy et al. [20]	External Torque Estimation	Coupled NN	MSE = 0.034677 RMSE = 0.18622	Torque sensor is required which is not available in industrial robots.
Mahmoud et al. [21]	External Torque Estimation	Recurrent NN	MSE = 0.03173 RMSE = 0.17813 R= 0.96797	Any industrial robot
G. d'Addato et al. [52]	Joint torques prediction	Cascaded NN	MSE= 2.2470e10−4	Any industrial robot
Tobias Gold et al. [53]	External Joint torque	Generalized Momentum Observer	RMSE = 2.75	Any industrial robot
Yanshu Song et al. [54]	Torque Estimation for Robotic Joint	Backpropagation NN	MSE or RMSE is not stated. Maximum error = 29.9Nm	Motor torque sensor is required which is not available in industrial robots.

(+) Note: Collaborative robot has both position and torque sensor at each joint, whereas industrial or conventional robot has only position sensor at each joint.

4. Discussion

This section gives a small discussion about the obtained results using Williams' method and using the proposed SVM-PSO. The proposed model for external torque prediction demonstrates robust predictive accuracy and generalization, as substantiated by multiple statistical and graphical evaluations. The use of the Williams plot was instrumental in delineating the model's applicability domain. Approximately 95% of the predictions from both the training and testing datasets fall within the standardized residual bounds of ±3 and the leverage threshold of H* = 0.0008, aligning with established benchmarks for model validity and reliability, [55]. This high proportion of well-fitted data points highlights the statistical robustness of the machine learning algorithm in prediction the torque of the joint [52] and consistent with previous studies where Williams plots effectively identified outliers in estimation or regression problems.

Although a small percentage of outliers are present in low-leverage regions, their presence highlights an inherent challenge in modeling complex nonlinear relationships, as also reported in earlier prediction frameworks using hybrid neural networks and fuzzy systems [56], [57]. These deviations, though limited in number, emphasize the potential benefit of integrating ensemble models or residual correction networks for improved performance at edge cases, as seen in [58].

The scatter plot and the corresponding error analysis (Fig. 10, Fig. 11) demonstrate a high level of agreement between actual and predicted torque values, with most predictions clustering closely around the ideal line. This pattern mirrors the observations of (Huo et al. [18]), who emphasized that a high prediction density along the regression line indicates stable learning and effective error minimization. The model's low MSE and RMSE values, remaining below 0.17 across phases, further support its stability, matching or exceeding performance benchmarks reported in related studies [59].

In addition, the small drop in R from 0.9952 (training) to 0.9862 (testing) suggests robust generalisation with little overfitting. This is significantly better than the results reported by [60], who reported R = 0.8923. The obtained results from the current study confirm the benefits of combining optimisation techniques such as PSO with machine learning models-a technique validated in multiple robotics and mechatronics applications [61], [62] .

Furthermore, the model's sensor-free construction or the model that needs only the internal position sensor at the robot's joint provides a substantial advantage for industrial applications. Some examples of previous techniques are such as those presented by C. B. Yigit et al. [63] and G. d'Addato et al. [52]. These techniques are depended on position sensor-based measurements and reported low error metrics, rendering them suitable for industrial robotic systems. Other methods such as Dimeas et al. [19] and Sharkawy et al. [20] require the torque sensor which renders them not suitable for general robotic systems. The current presented model in this paper retains high precision with an MAE of less than 0.06 without the need for external sensors-an important condition for widespread use in legacy robotic infrastructure, as emphasized by Mahmoud et al. [21] and G. d'Addato et al. [52].

Finally, our comparison analysis (Table 5) clearly shows that the suggested approach is at the forefront of torque estimating technologies. The combination of statistical precision, model transparency via residual diagnostics, and industrial compatibility confirms the method's viability for real-world deployment, meeting the dual goals of accuracy and practicality outlined in recent review literature [64].

5. Conclusion and Future Work

In this paper, we propose an optimized hybrid method for predicting the external torque of an industrial robotic manipulator. The method leverages three input features: (1) the current joint position error, (2) the previous joint position error, and (3) the actual joint velocity. The model's output is the estimated external torque at the corresponding joint. Experimental data were collected from the robotic manipulator under sinusoidal joint motion and some random collisions with the robot links. To assess the statistical quality of the dataset, Williams' method was applied to both training and testing sets, confirming consistent and reliable data behavior.

The performance evaluation of the proposed method during both training and testing phases demonstrates its effectiveness. In the training phase, the model achieved a RMSE of 0.0985 and a R of 0.9952, indicating excellent learning and accurate fitting. During testing, it maintained strong performance, with an RMSE of 0.1669 and $R = 0.986$, reflecting robust generalization to unseen data. Moreover, analysis of the convergence between the estimated and experimentally measured external torque further validates the model's high predictive capability.

To benchmark its performance, we conducted a comparative analysis against previously published external torque estimation methods. The results demonstrate that the proposed approach outperforms several state-of-the-art techniques in both accuracy and robustness. Moreover, the model relies solely on joint position and velocity inputs, eliminating the need for additional torque sensors-

thereby enhancing its applicability across a wide range of standard industrial and conventional robotic systems. Future works can be focused on the following points:

1) Including the acceleration as one of the inputs which is the primary driver of inertial torque. Then, investigating and comparing the performance of the model compared with current results.
2) Enhancing the model's performance through alternative training algorithms.
3) Exploring advanced deep learning techniques may offer further improvements in prediction accuracy and robustness, opening new avenues for high-precision, and real-time torque estimation in robotic applications.
4) Validating and testing the proposed model using a trajectory different from the training one. For example, the training is performed using sinusoidal motion and the testing is performed on a Pick-and-Place application.
5) Considering non-sinusoidal trajectories such as trapezoidal profile or random setpoints for training or testing the proposed model.
6) Applying the proposed method with multi-DOF Robot. For example, 3-DOF, 6-DOF, or 7-DOF robotic manipulators.

Data Availability Statement: The authors confirm that the data supporting the findings of this study are included within the article. More information can be requested from the corresponding author (Abdel-Nasser Sharkawy)

Author's Contributions: Conceptualization: IK, NB, AD, A.-N. S; methodology and software validation: IK, A.-N. S, AD; Data Curation: A.-N. S; formal analysis and writing-original draft: IK, A.-N. S, AD, LM; writing-review and editing: NB, A.-N. S; visualization: IK, NB, A.-N. S; Validation: A.-N. S; Project administration: A.-N. S. Most work done in this paper was carried out by Abdel-Nasser Sharkawy. All authors have read and agreed to the published version of the manuscript.

Funding: This research received no funding.

Acknowledgments: Not Applicable.

Declaration of Competing Interests: The authors declare that they have no known competing financial interests or personal relationships that could have appeared to influence the work reported in this paper.

Conflict of Interest: The authors declare no conflict of interest.

Abbreviations

Abbreviation	Meaning
SVM	Support vector machine
PSO	Particle swarm optimization
RMSE	Root mean squared error
MSE	Mean squared error
R	Regression (Correlation Coefficient)
DOF	Degree of freedom
H	Hat matrix
LWR	Light weight robot
MAE	Mean absolute error
NN	Neural network

Note: The order of these abbreviations is based on their appearance in the text of the paper.

References

[1] A. Keshvarparast, D. Battini, O. Battaia, and A. Pirayesh, "Collaborative robots in manufacturing and assembly systems: literature review and future research agenda," *Journal of Intelligent Manufacturing*, vol. 35, no. 5, pp. 2065-2118, 2024, https://doi.org/10.1007/s10845-023-02137-w.

[2] U. Othman and E. Yang, "Human–Robot Collaborations in Smart Manufacturing Environments: Review and Outlook," *Sensors*, vol. 23, no. 12, p. 5663, 2023, https://doi.org/10.3390/s23125663.

[3] H. Su, A. Di Lallo, R. R. Murphy, R. H. Taylor, B. T. Garibaldi, and A. Krieger, "Physical human–robot interaction for clinical care in infectious environments," *Nature Machine Intelligence*, vol. 3, no. 3, pp. 184-186, 2021, https://doi.org/10.1038/s42256-021-00324-z.

[4] I. N. Weerarathna, D. Raymond, and A. Luharia, "Human-Robot Collaboration for Healthcare: A Narrative Review," *Cureus*, vol. 15, no. 11, p. e49210, 2023, https://doi.org/10.7759/cureus.49210.

[5] H. Yu, S. Huang, G. Chen, Y. Pan and Z. Guo, "Human–Robot Interaction Control of Rehabilitation Robots With Series Elastic Actuators," *IEEE Transactions on Robotics*, vol. 31, no. 5, pp. 1089-1100, 2015, https://doi.org/10.1109/TRO.2015.2457314.

[6] A. Mohebbi, "Human-Robot Interaction in Rehabilitation and Assistance: a Review," *Current Robotics Reports*, vol. 1, no. 3, pp. 131-144, 2020, https://doi.org/10.1007/s43154-020-00015-4.

[7] H. Wang, N. Luo, T. Zhou, and S. Yang, "Physical Robots in Education: A Systematic Review Based on the Technological Pedagogical Content Knowledge Framework," *Sustainability*, vol. 16, no. 12, p. 4987, 2024, https://doi.org/10.3390/su16124987.

[8] M. Farajtabar and M. Charbonneau, "The path towards contact-based physical human–robot interaction," *Robotics and Autonomous Systems*, vol. 182, p. 104829, 2024, https://doi.org/10.1016/j.robot.2024.104829.

[9] C. S. Song and Y. K. Kim, "The role of the human-robot interaction in consumers' acceptance of humanoid retail service robots," *Journal of Business Research*, vol. 146, pp. 489-503, 2022, https://doi.org/10.1016/j.jbusres.2022.03.087.

[10] B. Cagiltay, "Designing for In-Home Long-Term Family-Robot Interactions: Family Preferences, Connection-Making, and Privacy," *Conference on Human Factors in Computing Systems - Proceedings*, pp. 1-6, 2023, https://doi.org/10.1145/3544549.3577035.

[11] I. Maurtua, A. Ibarguren, J. Kildal, L. Susperregi, and B. Sierra, "Human-robot collaboration in industrial applications: Safety, interaction and trust," *International Journal of Advanced Robotic Systems*, vol. 14, no. 4, pp. 1-10, 2017, https://doi.org/10.1177/1729881417716010.

[12] M. Hamad, S. Nertinger, R. J. Kirschner, L. Figueredo, A. Naceri, and S. Haddadin, "A Concise Overview of Safety Aspects in Human-Robot Interaction," *Human-Friendly Robotics 2023*, pp. 1-18, 2024, https://doi.org/10.1007/978-3-031-55000-3_1.

[13] A. N. Sharkawy, K. H. Mahmoud, and G. T. Abdel-jaber, "Ensuring Safety in Human-Robot Cooperation: Key Issues and Future Challenges," *Control Systems and Optimization Letters*, vol. 2, no. 3, pp. 274-284, 2024, https://doi.org/10.59247/csol.v2i3.154.

[14] A.-N. Sharkawy and P. N. Koustoumpardis, "Human–Robot Interaction: A Review and Analysis on Variable Admittance Control, Safety, and Perspectives," *Machines*, vol. 10, no. 7, p. 591, 2022, https://doi.org/10.3390/machines10070591.

[15] L. D. Phong, J. Choi and S. Kang, "External force estimation using joint torque sensors for a robot manipulator," *2012 IEEE International Conference on Robotics and Automation*, pp. 4507-4512, 2012, https://doi.org/10.1109/ICRA.2012.6224977.

[16] L. Roveda, D. Riva, G. Bucca and D. Piga, "External Joint Torques Estimation for a Position-Controlled Manipulator Employing an Extended Kalman Filter," *2021 18th International Conference on Ubiquitous Robots (UR)*, pp. 101-107, 2021, https://doi.org/10.1109/UR52253.2021.9494674.

[17] N. Likar and L. Žlajpah, "External joint torque-based estimation of contact information," *International Journal of Advanced Robotic Systems*, vol. 11, no. 1, 2014, https://doi.org/10.5772/58834.

[18] Z. Huo, M. Yuan, S. Zhang, and X. Zhang, "Observer-Based Adaptive Robust Force Control of a Robotic Manipulator Integrated with External Force/Torque Sensor," *Actuators*, vol. 14, no. 3, p. 116, 2025, https://doi.org/10.3390/act14030116.

[19] F. Dimeas, L. D. Avendaño-Valencia, and N. Aspragathos, "Human - Robot collision detection and identification based on fuzzy and time series modelling," *Robotica*, vol. 33, no. 9, pp. 1886-1898, 2015, https://doi.org/10.1017/S0263574714001143.

[20] A. N. Sharkawy, P. N. Koustoumpardis, and N. Aspragathos, "Human-robot collisions detection for safe human-robot interaction using one multi-input-output neural network," *Soft Computing*, vol. 24, no. 9, pp. 6687-6719, 2020, https://doi.org/10.1007/s00500-019-04306-7.

[21] K. H. Mahmoud, A. N. Sharkawy, and G. T. A. Jaber, "Development of safety method for a 3-DOF industrial robot based on recurrent neural network," *Journal of Engineering and Applied Science*, vol. 70, no. 44, pp. 1-20, 2023, https://doi.org/10.1186/s44147-023-00214-8.

[22] T. Zhang *et al*., "A novel joint external torque estimate model of the lightweight robot's joint based on a BP neural network," *Robotica*, vol. 43, no. 3, pp. 1027-1042, 2025, https://doi.org/10.1017/S0263574725000086.

[23] R. M. Murray, Z. Li, and S. S. Sastry, "A Mathematical Introduction to Robotic Manipulation," *CRC Press*, 1994, https://books.google.co.id/books/about/A_Mathematical_Introduction_to_Robotic_M.html?id=D_PqGKRo7oIC&redir_esc=y.

[24] A. N. Sharkawy and P. N. Koustoumpardis, "Dynamics and computed-torque control of a 2-DOF manipulator: Mathematical analysis," *International Journal of Advanced Science and Technology*, vol. 28, no. 12, pp. 201-212, 2019, https://hal.science/hal-03598924/.

[25] C. Cho, J. Kim, Y. Kim, J.-B. Song, and J.-H. Kyung, "Collision Detection Algorithm to Distinguish Between Intended Contact and Unexpected Collision," *Advanced Robotics*, vol. 26, no. 16, pp. 1825-1840, 2012, https://doi.org/10.1080/01691864.2012.685259.

[26] B. Jung, J. C. Koo, H. R. Choi, and H. Moon, "Human-robot collision detection under modeling uncertainty using frequency boundary of manipulator dynamics," *Journal of Mechanical Science and Technology*, vol. 28, no. 11, pp. 4389-4395, 2014, https://doi.org/10.1007/s12206-014-1006-5.

[27] F. Min, G. Wang, and N. Liu, "Collision Detection and Identification on Robot Manipulators Based on Vibration Analysis," *Sensors*, vol. 19, no. 5, p. 1080, 2019, https://doi.org/10.3390/s19051080.

[28] M. Indri, S. Trapani, and I. Lazzero, "Development of a Virtual Collision Sensor for Industrial Robots," *Sensors*, vol. 17, no. 5, p. 1148, 2017, https://doi.org/10.3390/s17051148.

[29] Shujun Lu, J. H. Chung and S. A. Velinsky, "Human-Robot Collision Detection and Identification Based on Wrist and Base Force/Torque Sensors," *Proceedings of the 2005 IEEE International Conference on Robotics and Automation*, pp. 3796-3801, 2005, https://doi.org/10.1109/ROBOT.2005.1570699.

[30] A. C. Smith and K. Hashtrudi-Zaad, "Application of neural networks in inverse dynamics based contact force estimation," *Proceedings of 2005 IEEE Conference on Control Applications, 2005. CCA 2005.*, pp. 1021-1026, 2005, https://doi.org/10.1109/CCA.2005.1507264.

[31] H. D. Patino, R. Carelli and B. R. Kuchen, "Neural networks for advanced control of robot manipulators," *IEEE Transactions on Neural Networks*, vol. 13, no. 2, pp. 343-354, 2002, https://doi.org/10.1109/72.991420.

[32] K. Y. Goldberg and B. A. Pearlmutter, "Using a neural network to learn the dynamics of the CMU Direct-Drive Arm II," *Carnegie Mellon University*, 1988, https://kilthub.cmu.edu/ndownloader/files/12105260.

[33] D. J. Sebald and J. A. Bucklew, "Support vector machine techniques for nonlinear equalization," *IEEE Transactions on Signal Processing*, vol. 48, no. 11, pp. 3217-3226, 2000, https://doi.org/10.1109/78.875477.

[34] J. A. K. Suykens, "Support Vector Machines: A Nonlinear Modelling and Control Perspective," *European Journal of Control*, vol. 7, no. 2-3, pp. 311-327, 2013, https://doi.org/10.3166/ejc.7.311-327.

[35] A. Dahmani, Y. Ammi, and S. Hanini, "A Novel Non-Linear Model Based on Bootstrapped Aggregated Support Vector Machine for the Prediction of Hourly Global Solar Radiation," *Smart Grids and Sustainable Energy*, vol. 9, no. 3, 2023, https://doi.org/10.1007/s40866-023-00179-w.

[36] A. Shrotriya, C. Nayak, G. Patel, M. I. Khan, and V. K. Pathak, "A new method based on AVOA-optimized support vector machine for predicting performance characterisitcs during turning aluminium 7068 under graphene nanofluid," *Scientific Reports*, vol. 16, 2026, https://doi.org/10.1038/s41598-025-32577-8.

[37] H. M. Omran, K. Ibrahim, G. T. Abdel-jaber, and A.-N. Sharkawy, "Brain Tumor Classification from MRI Images Using Hybrid Deep Learning Approaches: VGG19 with SoftMax and SVM Classifiers," *International Journal of Robotics and Control Systems*, vol. 6, no. 1, pp. 16-35, 2026, https://doi.org/10.31763/ijrcs.v6i1.2260.

[38] A. Dahmani *et al*., "Assessing the Efficacy of Improved Learning in Hourly Global Irradiance Prediction," *Computers, Materials & Continua*, vol. 77, no. 2, pp. 2579-2594, 2023, https://doi.org/10.32604/cmc.2023.040625.

[39] K. Ikram, K. Djilali, D. Abdennasser, R. Al-Sabur, B. Ahmed, and A. N. Sharkawy, "Comparative analysis of fouling resistance prediction in shell and tube heat exchangers using advanced machine learning techniques," *Research on Engineering Structures & Materials*, vol. 10, no. 1, pp. 253-270, 2024, http://dx.doi.org/10.17515/resm2023.858en0816.

[40] A. Srivastava and S. K. Parida, "A Robust Fault Detection and Location Prediction Module Using Support Vector Machine and Gaussian Process Regression for AC Microgrid," *IEEE Transactions on Industry Applications*, vol. 58, no. 1, pp. 930-939, 2022, https://doi.org/10.1109/TIA.2021.3129982.

[41] W. Niu, Z. Feng, B. Feng, Y. Min, and C. Cheng, "Neural Network, Extreme Learning Machine, and Support Vector Machine in Deriving Operation Rule of Hydropower Reservoir," *Water*, vol. 11, no. 1, p. 88, 2019, https://doi.org/10.3390/w11010088.

[42] R. Nariswari and H. Pudjihastuti, "Support Vector Machine Method for Predicting Non-Linear Data," *Procedia Computer Science*, vol. 227, pp. 884-891, 2023, https://doi.org/10.1016/j.procs.2023.10.595.

[43] J. Kennedy and R. Eberhart, "Particle swarm optimization," *Proceedings of ICNN'95 - International Conference on Neural Networks*, vol. 4, pp. 1942-1948, 1995, https://doi.org/10.1109/ICNN.1995.488968.

[44] Z. Jiang, D. Zhu, X.-Y. Li, and L.-B. Han, "A Hybrid Adaptive Particle Swarm Optimization Algorithm for Enhanced Performance," *Applied Sciences*, vol. 15, no. 11, p. 6030, 2025, https://doi.org/10.3390/app15116030.

[45] S. Du, "Improved Multi-Objective Particle Swarm Optimization for Sustainable Building Design," *Journal of Engineering, Project, and Production Management*, vol. 16, no. 1, pp. 1-12, 2026, http://www.ppml.url.tw/EPPM_Journal/volumns/16_01_January_2026/ID_2025-155.pdf#.

[46] J. Du, Y. Liu, Y. Yu, and W. Yan, "A prediction of precipitation data based on Support Vector Machine and Particle Swarm Optimization (PSO-SVM) algorithms," *Algorithms*, vol. 10, no. 2, p. 57, 2017, https://doi.org/10.3390/a10020057.

[47] A. Dahmani *et al*., "Enhanced hourly temperature prediction using advanced ensemble neural networks for energy system efficiency optimization in hyper-arid regions," *AIP Advances*, vol. 15, no. 4, p. 045019, 2025, https://doi.org/10.1063/5.0257671.

[48] M. Hamadache, O. Benkortbi, S. Hanini, and A. Amrane, "QSAR modeling in ecotoxicological risk assessment: application to the prediction of acute contact toxicity of pesticides on bees (Apis mellifera L.)," *Environmental Science and Pollution Research*, vol. 25, pp. 896-907, 2018, https://doi.org/10.1007/s11356-017-0498-9.

[49] A. Dahmani, "Contribution à la modélisation de l'irradiation solaire par l'intelligence artificielle. Etude comparative," *Dspace Relizane University*, 2024, http://dspace.univ-relizane.dz/home/handle/123456789/536.

[50] A. Dahmani *et al*., "Parametric Analysis of Climate Factors for Monthly Weather Prediction in Ghardaïa District Using Machine Learning-Based Approach: ANN-MLPs," *International Journal of Robotics and Control Systems*, vol. 5, no. 1, pp. 179-196, 2025, https://doi.org/10.31763/ijrcs.v5i1.1651.

[51] R. Bischoff *et al*., "The KUKA-DLR Lightweight Robot arm - a new reference platform for robotics research and manufacturing," *ISR 2010 (41st International Symposium on Robotics) and ROBOTIK 2010 (6th German Conference on Robotics)*, pp. 1-8, 2010, https://ieeexplore.ieee.org/abstract/document/5756872.

[52] G. d'Addato, R. Carli, E. Pedrosa, A. Pereira, L. Palopoli, and D. Fontanelli, "Joint torques prediction of a robotic arm using neural networks," *arXiv*, 2024, https://doi.org/10.48550/arXiv.2405.00695.

[53] T. Gold, A. Völz, and K. Graichen, "External torque estimation for an industrial robot arm using joint torsion and motor current measurements," *IFAC-PapersOnLine*, vol. 52, no. 15, pp. 352-357, 2019, https://doi.org/10.1016/j.ifacol.2019.11.700.

[54] Y. Song, H. Huang, F. Liu, F. Xi, D. Zhou and B. Li, "Torque Estimation for Robotic Joint With Harmonic Reducer Based on Deformation Calibration," *IEEE Sensors Journal*, vol. 20, no. 2, pp. 991-1002, 2020, https://doi.org/10.1109/JSEN.2019.2944975.

[55] C. Trinh, Y. Tbatou, S. Lasala, O. Herbinet, and D. Meimaroglou, "On the development of descriptor-based machine learning models for thermodynamic properties: Part 1-from data collection to model construction: understanding of the methods and their effects," *Processes*, vol. 11, no. 12, p. 3325, 2023, https://doi.org/10.3390/pr11123325.

[56] F. Ododo and N. Addotey, "Understanding the Influence of Outliers on Machine Learning Model Interpretability," *International Journal of African Sustainable Development Research*, vol. 7, no. 2, pp. 41-58, 2025, https://doi.org/10.70382/tijasdr.v07i2.019.

[57] G. Boukhalfa, S. Belkacem, A. Chikhi, and S. Benaggoune, "Genetic algorithm and particle swarm optimization tuned fuzzy PID controller on direct torque control of dual star induction motor," *Journal of Central South University*, vol. 26, no. 7, pp. 1886-1896, 2019, https://doi.org/10.1007/s11771-019-4142-3.

[58] P. Yue, B. Xu, and M. Zhang, "An improve nonlinear robust control approach for robotic manipulators with PSO-based global optimization strategy," *Scientific Reports*, vol. 14, no. 1, p. 21447, 2024, https://doi.org/10.1038/s41598-024-72156-x.

[59] W. Nawae and K. Thongpull, "PMSM Torque Estimation Based on Machine Learning Techniques," *2020 International Conference on Power, Energy and Innovations (ICPEI)*, pp. 137-140, 2020, https://doi.org/10.1109/ICPEI49860.2020.9431433.

[60] A.-N. Sharkawy and M. M. Ali, "NARX neural network for safe human–robot collaboration using only joint position sensor," *Logistics*, vol. 6, no. 4, p. 75, 2022, https://doi.org/10.3390/logistics6040075.

[61] Q. Li, P. Zeng, Q. Wu, and Z. Zhang, "RAPSO: An Integrated PSO with Reinforcement Learning and an Adaptive Weight Strategy for the High-Precision Milling of Elastic Materials," *Sensors*, vol. 25, no. 18, p. 5913, 2025, https://doi.org/10.3390/s25185913.

[62] Q. Chang *et al*., "A Data-Driven Method for Predicting and Optimizing Industrial Robot Energy Consumption Under Unknown Load Conditions," *Actuators*, vol. 13, no. 12, p. 516, 2024, https://doi.org/10.3390/act13120516.

[63] C. B. Yigit, E. Bayraktar, O. Kaya and P. Boyraz, "External Force/Torque Estimation With Only Position Sensors for Antagonistic VSAs," *IEEE Transactions on Robotics*, vol. 37, no. 2, pp. 675-682, 2021, https://doi.org/10.1109/TRO.2020.3031268.

[64] M. Y. Cao, S. Laws and F. R. y. Baena, "Six-Axis Force/Torque Sensors for Robotics Applications: A Review," *IEEE Sensors Journal*, vol. 21, no. 24, pp. 27238-27251, 2021, https://doi.org/10.1109/JSEN.2021.3123638.